Systems & Control Transactions

Research Article - Peer Reviewed Conference Proceeding
ESCAPE 35 - European Symposium on Computer Aided Process Engineering
Ghent, Belgium. 6-9 July 2025
Jan F.M. Van Impe, Grégoire Léonard, Satyajeet S. Bhonsale,
Monika E. Polańska, Filip Logist (Eds.)

PSE PRESS

Process simulation and thermodynamic analysis of newly synthesized pre-combustion CO_2 capture system using novel Ionic liquids for H_2 production

Sadah Mohammed[a], Fadwa Eljack[a]*

[a] Qatar University, Department of Chemical Engineering, College of Engineering, P.O. Box 2713, Doha, Qatar
*Corresponding Author: Fadwa.Eljack@qu.edu.qa

ABSTRACT

This paper evaluates the thermodynamic efficiency of a newly synthesized large-scale pre-combustion CO_2 capture process using a novel ionic liquid (IL) 1-octyl-2,3-methylimidazolium thiocyanate [OMMIM][SCN] for blue H_2 production. In addition, the potential eco-toxicity of the selected IL was assessed using the ADMETlab 2.0 web tool. The results of these analyses were compared to those of an established IL 1-butyl-2,3-dimethylimidazolium bis(trifluoromethyl sulfonyl)imide [BMMIM][TF2N]. The eco-toxicity assessment confirmed that [OMMIM][SCN] is less environmentally toxic than [BMMIM][TF2N]. Thermodynamic analysis of the novel system shows the COOLER unit accounts for the highest energy demand; however, the [OMMIM][SCN] system demonstrates a 7.45% reduction in energy consumption in the COOLER unit compared to [BMMIM][TF2N]. The system experienced the highest exergy losses (irreversibilities) in the COOLER unit for [BMMIM][TF2N] (12982 kW) and in the flash separator unit for [OMMIM][SCN] (8256 kW). The thermodynamic efficiency was analyzed within a specified IL inlet temperature range (25°C – 75°C) and absorption pressure range (7 - 16 bar). The results show that the [OMMIM][SCN] system outperforms [BMMIM][TF2N] with higher IL inlet temperature but decreases at higher absorption pressure, while [BMMIM][TF2N] maintains constant energy efficiency. The exergy efficiency of the [OMMIM][SCN] system shows better performance across the studied conditions but decreases beyond the peak temperature range of 50–60°C. These findings highlight the potential of [OMMIM][SCN] as an excellent alternative solvent for pre-combustion CO_2 capture applications.

Keywords: Hydrogen, Carbon Dioxide Capture, Energy Efficiency, Exergy Efficiency, Aspen Plus

INTRODUCTION

Hydrogen (H_2), a non-carbonaceous fuel abundant on earth in its oxidized form, has emerged as a promising pathway for deep decarbonization in various sectors, such as power generation and transportation [1]. However, the majority of the H_2 is produced from reforming fossil fuels, with steam methane reforming (SMR) accounting for 50% of the total production, without carbon capture, resulting in high CO_2 emissions (89.1 gCO_2/MJ) [2]. Blue H_2 is a viable solution with lower carbon intensity (22.4 gCO_2/MJ) and offers a feasible route to sustain reliance on fossil fuels [3]. Therefore, developing an economically viable and sustainable CO_2 capture system with a low environmental footprint is imperative. The pre-combustion CO_2 capture system has been widely explored in H_2 production units for its effectiveness in handling high-pressure streams with high CO_2 concentrations. In this context, solvent selection is essential for designing the CO_2 removal system by considering various factors, encompassing eco-toxicity, minimizing irreversibility, and increasing energy efficiency. Ionic liquids (ILs) have shown exceptional performance in reducing energy regeneration compared to conventional solvents such as Monoethanolamine (MEA), making ILs well-suited for pre-combustion applications [4]. Nevertheless, their tunability makes it challenging to synthesize the optimal IL from numerous possibilities.

This work conducts a comprehensive thermodynamic analysis of a newly synthesized pre-combustion

CO_2 capture process for large-scale H_2 production. The analysis aims to evaluate its energy and exergy performance and identify process irreversibilities. A novel IL 1-octyl-2,3-methylimidazolium thiocyanate [OMMIM][SCN], designed in our previous work using a predictive deep learning model [5], was utilized as a physical absorbent in this study (see **Figure 1**). The IL was defined in the simulation software Aspen Plus, following the integrated modified translation-rotation-internal coordinate (TRIC) system with the COSMO-based/Aspen approach developed in our previous work [6]. An eco-toxicity analysis was carried out using the ADMETlab 2.0 web tool [7] to evaluate the environmental suitability of [OMMIM][SCN]. Finally, the performance of [OMMIM][SCN] was compared to an established IL, 1-butyl-2,3-dimethylimidazolium bis(trifluoromethyl sulfonyl)imide [BMMIM][TF2N] to assess their relative effectiveness in the process and their environmental suitability.

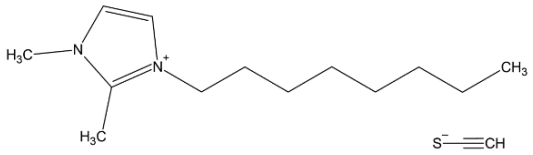

Figure 1. Molecular structure of novel IL [OMMIM][SCN] [5]

METHODOLOGY

Eco-Toxicity assessment

The ADMETlab 2.0 web tool evaluated the selected ILs' eco-toxicity, leveraging its robust framework for accurate toxicity predictions. By providing the SMILES (Simplified Molecular Input Line Entry System) representation of the IL as input to the platform, the molecular structure is processed to predict different properties using the advanced quantitative structure-property relationship (QSPR) model. The platform assesses different endpoints, such as environmental toxicity. It evaluates carcinogenicity, eye and skin irritation, and respiratory toxicity. The results of the assessment are shown as numerical scores. These scores range from 0 to 1 and then are categorized using an empirical decision scale, as indicated in **Table 1**.

Table 1: Empirical decision score based on ADMETlab 2.0 framework [7].

Empirical decision	Category
0.0-0.3	"Non-toxic"
0.3-0.7	"Slightly toxic"
0.7-1.0	"Toxic"

Large-scale pre-combustion CO_2 capture simulation

Following the TRIC system with the COSMO-based/Aspen approach, the novel IL [OMMIM][SCN] was successfully defined in the simulation software Aspen Plus V12 as a pseudocomponent. A steady-state large-scale pre-combustion CO_2 capture process was then developed, as depicted in **Figure 2**. This process was designed to capture 90% of the CO_2 and achieve an H_2 purity of 97%. It treats H_2 produced from a large-scale steam methane reformer (SMR), generating a 6.98x104 kg/h flow of syngas stream with the following compositions: 16.27% CO_2, 4.63% CO, 75.61% H_2, 3.05% CH_4, 0.24% H_2O, and 0.2% N_2. The syngas flow specifications were obtained from the IEAGHG report [8]. The proposed configuration comprises four main components: absorption columns, pumps, flash drums, heat exchangers, and compressors. The process specifications suggested by Hospital-Benito et al.[9], were used to develop the large-scale pre-combustion process in Aspen Plus. During the process development, the number of stages was adjusted and it was only 10 stages required to achieve the specified CO_2 removal target of (90%).

The syngas stream enters a flash separator (F-101) to separate the water content from the gas stream. The dry gas stream (S4) then enters a "RADFRAC" packed bed absorber column at 35°C and 26 bar, where the CO_2 is absorbed by the IL counter currently within the column. The stream "PURE H_2" exists from the column overhead, whereas the CO_2-rich stream (S6) leaves from the bottom of the column and enters the flash drum (F-102) to remove and recycle H_2 back to the absorber. Before the regeneration stage, the CO_2-rich stream (S8) is heated by a heat exchanger (HEATER) to a temperature suitable for effective separation. Then, the heated stream (S9) enters two flash separators arranged in series for the regeneration of IL, where the streams that contain mostly CO_2 leave the top of the flash columns (F-103 and F-104) and are combined via a mixer (M-102). The regenerated IL (S15) from F-104 is cooled via a heat exchanger (COOLER) and recirculated back (LEANIN) to the absorber.

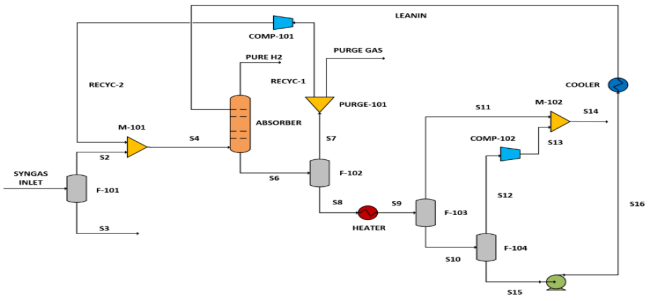

Figure 2. Large-scale pre-combustion CO_2 capture process scheme

Energy and exergy analysis

Evaluating the thermodynamic efficiency via process system engineering aspects, such as energy and exergy, is essential for optimizing pre-combustion CO_2 capture and achieving maximum CO_2 capture efficiency and H_2 purity.

The energy-consuming equipment in the suggested process scheme includes heat exchangers, compressors, and flash separators. The equipment's energy duty (kW) values were obtained from Aspen Plus.

The overall thermal efficiency (η) of the CO_2 capture process can be evaluated using equation (1) [10]:

$$\eta = \frac{\sum \dot{Q}_{useful} + \sum \dot{W}_{out} + \sum \dot{m}_{useful} h_{useful}}{\sum \dot{Q}_{in} + \sum \dot{W}_{in} + \sum \dot{m}_{in} h_{in}} \quad (1)$$

Where $\dot{Q}_{useful}$ is the useful thermal energy output, $\dot{W}_{out}$ refers to the useful mechanical energy output, $\dot{Q}_{in}$ and $\dot{W}_{in}$ represent the total thermal energy and the mechanical energy inputs to the system, respectively, $\dot{m}_{useful}$ indicates the mass flow rate of useful products, specifically the pure H_2 stream, and the captured CO_2, $\dot{m}_{in}$ refers to the inlet mass flow rate, h_{useful} and h_{in} represent the enthalpy of useful and input streams, respectively.

The exergy flow rate $\dot{E}x$ of a material stream can be calculated using equation (2) [10]:

$$\dot{E}x = \dot{m}[(h_i - h_o) - T_o(s_i - s_o)] \quad (2)$$

h_i and s_i denote the stream's specific molar enthalpy and entropy in a certain state, h_o and s_o refer to specific molar enthalpy and entropy in the reference state (T_o = 25°C, P_o = 1 bar), and T_o represents the reference temperature. The exergy destruction rate ($\dot{E}x_d$) can be calculated from the exergy balance equation of the main processing equipment as given by equation (3) [10]:

$$\sum \dot{m}_{in}\dot{E}x_{in} + Q_{consumption}\left(1 - \frac{T_o}{T}\right) + \dot{W}_{consumption} = \sum \dot{m}_{out}\dot{E}x_{out} + \dot{Q}_{generation}\left(1 - \frac{T_o}{T}\right) + \dot{W}_{generation} + \dot{E}x_d \quad (3)$$

Where the term $Q\left(1 - \frac{T_o}{T}\right)$ denotes the rate of exergy destruction associated with heat transfer. $\dot{E}x_{in}$ and $\dot{E}x_{out}$ refer to the inlet and outlet exergy flow rate mass, $\dot{E}x_d$ is the exergy destruction, $\dot{W}_{consumption}$ work consumed by the system, and $\dot{W}_{generation}$ generated by the system

The overall exergy efficiency of the proposed process configuration can be calculated using equation (4) [10]:

$$\varepsilon = \frac{\sum Ex(\dot{Q}_{useful}) + \sum \dot{W}_{out} + \sum \dot{m}_{useful} Ex_{useful}}{\sum Ex(\dot{Q}_{in}) + \sum \dot{W}_{in} + \sum \dot{m}_{in} Ex_{in}} \quad (4)$$

RESULTS AND DISCUSSION

Eco-toxic evaluation of selected ILs

The toxicity evaluation for both ILs, [OMMIM][SCN] and [BMMIM][TF2N], was conducted using the ADMETlab 2.0 web tool. The results of the assessment are summarized in Table 2. The toxicological profiles of IL [OMMIM][SCN] and [BMMIM][TF2N] differ noticeably. For instance, [OMMIM][SCN] is classified as slightly toxic for carcinogenicity (0.478), whereas [BMMIM][TF2N] is toxic (0.944), indicating a higher risk. However, despite these differences, both ILs exhibit high toxicity in respiratory effect, with [BMMIM][TF2N] demonstrating a slightly higher value (0.986) compared to [OMMIM][SCN] (0.882). Overall, the newly designed IL [OMMIM][SCN] shows less toxicity across multiple properties, suggesting that the IL is relatively safer and environmentally suitable.

Table 2: Probability of eco-toxicity assessment parameters

Property	[OMMIM][SCN]	[BMMIM][TF2N]
Carcinogenicity	0.478 (slightly toxic)	0.944 (toxic)
Eye Corrosion	0.257 (nontoxic)	0.003 (nontoxic)
Eye Irritation	0.434 (slightly toxic)	0.032 (nontoxic)
Skin Sensitization	0.156 (nontoxic)	0.325 (slightly toxic)
Respiratory Toxicity	0.882 (toxic)	0.986 (toxic)

Thermodynamic analysis

The energy performance of the large-scale pre-combustion CO_2 capture process was analyzed, targeting a 90% CO_2 removal rate, and the results are shown in **Figure 3**. The COOLER demonstrates the highest energy demand for both ILs, with the [OMMIM][SCN] system requiring slightly less energy by 7.45% (33985 kW) than [BMMIM][TF2N] (36722 kW). On the other hand, the energy consumption associated with the HEATER, P-101, Comp-101, and Comp-102 is nearly identical for the two ILs. A noticeable difference is observed in energy demand for F-104, where [OMMIM][SCN], at 1080 kW, requires less energy than [BMMIM][TF2N] (2743 kW). In contrast, the total energy demand in F-102 (4785 kW) is slightly larger for [OMMIM][SCN] compared to [BMMIM][TF2N] (3748 kW).

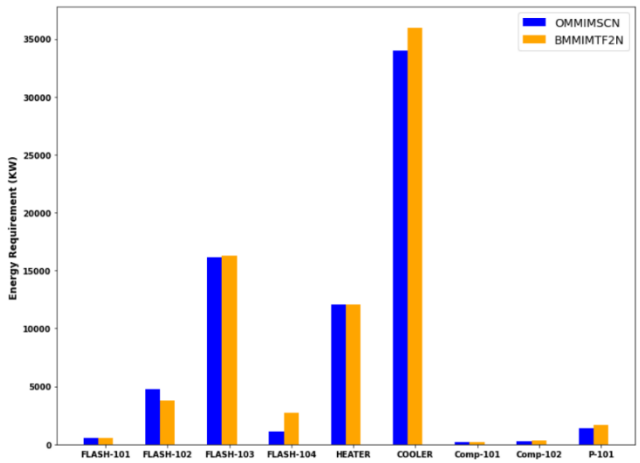

Figure 3. Comparisons of energy requirement for different equipment for both ILs.

Each unit's irreversibility (exergy loss) is calculated using equations (2) and (3), and the results are highlighted in **Figure 4**. The analysis shows that in the [BMMIM][TF2N] system, the COOLER component is the largest contributor to exergy loss, accounting for 47% (12982 kW) of the total exergy loss of the entire system. Conversely, the energy destruction in the [OMMIM][SCN] system is much lower (4690 kW), indicating that [OMMIM][SCN] operates with higher thermodynamic efficiency in the COOLER unit. In the separation stage (C-101), exergy loss in the [OMMIM][SCN] system is higher at 4048 kW compared to 2431 kW for the [BMMIM][TF2N] system. As for the regeneration stage, the exergy loss is greater in both units F-102 (1383 kW) and F-103 (8256 kW) in the [OMMIM][SCN] system compared to [BMMIM][TF2N], while [OMMIM][SCN] experiences less exergy loss in F-104, at 646 kW, than [BMMIM][TF2N] system.

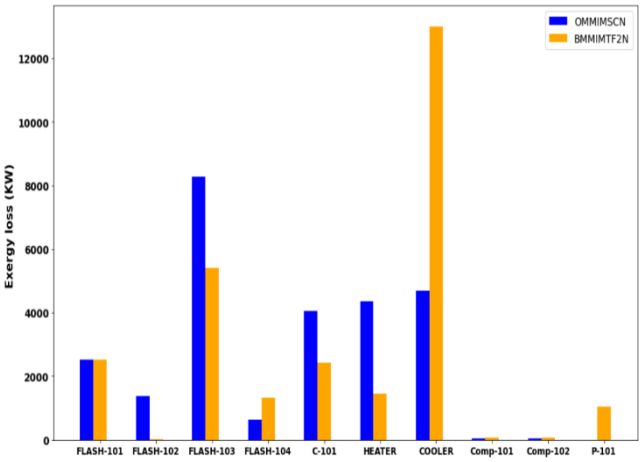

Figure 4. Exergy loss comparison across various equipment for both ILs.

Parametric analysis

This section examines the impact of system parameters like the IL inlet temperature and absorption pressure on the thermodynamic efficiency of the proposed pre-combustion CO_2 capture process configuration. The effect was studied within the temperature range of 25°C to 75°C and pressure absorption range of 7 to 22 bar and 7 to 16 bar for energy and exergy efficiency, respectively.

Effect of IL inlet temperature

Using equation (1), the total energy efficiency of the entire process was calculated within the specified temperature range, and the result is depicted in **Figure 5**. The system's energy efficiency decreases as the inlet temperature increases. The highest energy efficiency for both systems, [OMMIM][SCN] and [BMMIM][TF2N], occurs at 25°C. However, [OMMIM][SCN] demonstrates higher energy efficiency (91.2%) at 25°C than [BMMIM][TF2N] (90.6%). Additionally, the difference in energy efficiency between the two systems decreases across the temperature range, with the [OMMIM][SCN] system achieving higher energy efficiency. This trend continues throughout the temperature range, suggesting that the [OMMIM][SCN] system consumes less energy and, therefore, is more energy-efficient.

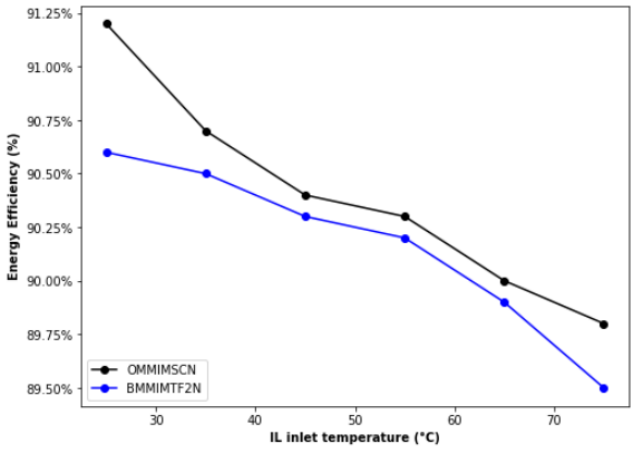

Figure 5. Effect of IL inlet temperautre on Energy Efficiecny (%).

Equations (2), (3), and (4) are used to calculate the overall exergy efficiency. **Figure 6** illustrates the exergy efficiency for both systems across the specified range for IL inlet temperature. As depicted from the graph, both IL systems demonstrate a significant increase in exergy efficiency as the temperature rises. The [OMMIM][SCN] system exhibited a higher exergy efficiency than [BMMIM][TF2N] throughout the temperature range, indicating that the [OMMIM][SCN] system experiences fewer irreversibilities. The maximum exergy efficiency occurs at 50-60°C, where [OMMIM][SCN] has slightly higher exergy efficiency (73.24%) compared to [BMMIM][TF2N]

(71.1%). Beyond this optimal range, the efficiency declines for both systems to around 57% at 75°C.

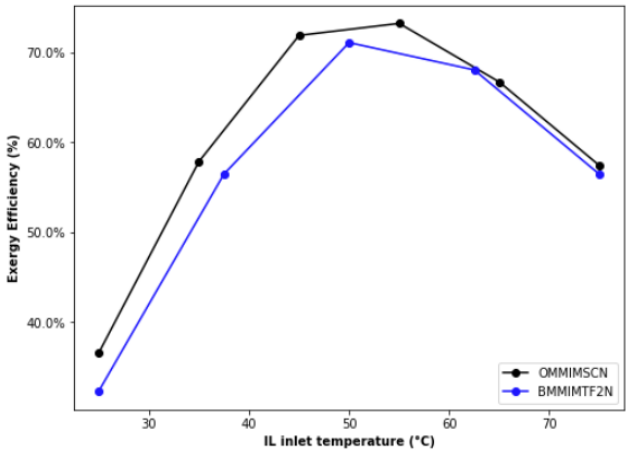

Figure 6. Effect of IL inlet temperautre on Exergy Efficiecny (%).

Effect of absorption pressure

The impact of varying the absorption pressure on the overall energy efficiency was also calculated. As seen in **Figure 7**, the [OMMIM][SCN] system demonstrates a decline in efficiency as the pressure increases, whereas [BMMIM][TF2N] maintains energy efficiency close to 89.9% throughout the pressure range. While, [OMMIM][SCN] shows higher energy efficiency (91%) at 7 bar compared to [BMMIM][TF2N] (89.9%), the efficiency of [OMMIM][SCN] decreases by 1% within the limited pressure range of 10-16 bar. Given that physical absorption generally favors higher pressures for better CO_2 removal, [BMMIM][TF2N] is more suitable for higher absorption pressures.

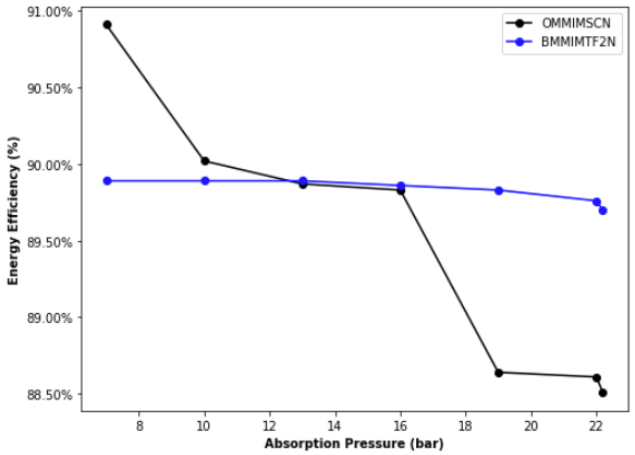

Figure 7. Effect of absorption pressure on Energy Efficiency (%)

Similarly, the parametric analysis was conducted to calculate the exergy efficiency within the specified pressure range. As illustrated in **Figure 8**, both IL systems experience a significant increase in efficiency as the pressure rises. The [OMMIM][SCN] system achieves higher efficiency across the pressure range compared to [BMMIM][TF2N], increasing from 25% to 37%. In contrast, the exergy efficiency for [BMMIM][TF2N] increases from 21% to 33%.

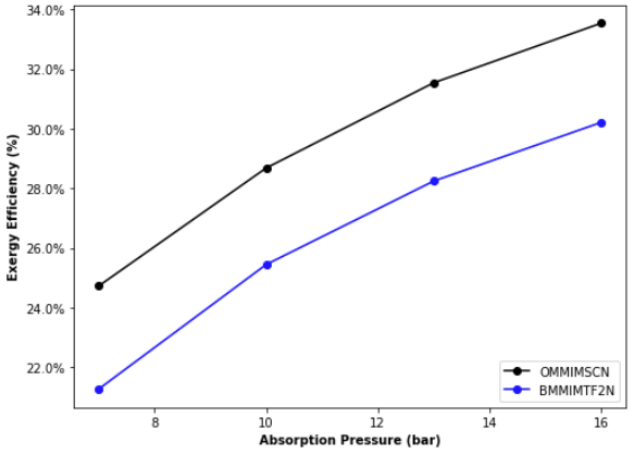

Figure 8. Effect of absorption pressure on Exergy Efficiency (%)

CONCLUSIONS

This study evaluates the thermodynamic efficiency of a large-scale pre-combustion CO_2 capture process using two IL systems: novel IL [OMMIM][SCN] and established IL [BMMIM][TF2N]. Alongside the thermodynamic performance, the toxicity analysis of ILs using ADMETlab 2.0 was evaluated. The results indicate that [OMMIM][SCN] is less toxic across the studied properties, indicating that the IL is environmentally safer compared to [BMMIM][TF2N]. The results of the thermodynamic analysis conducted at a 90% CO_2 removal rate reveal that the highest energy consumption for both IL systems occurs at the “COOLER” units, while [BMMIM][TF2N] requires slightly more energy duty. Moreover, the “F-104” exhibits a larger energy demand in the [BMMIM][TF2N] system, whereas the energy consumption for [OMMIM][SCN] is marginally larger in “F-102”. Similarly, the exergy destruction results demonstrate that the “COOLER” in the [BMMIM][TF2N] contributes the highest system irreversibility. Conversely, [OMMIM][SCN] experiences higher exergy loss in F-102 and F-103 compared to [BMMIM][TF2N]. In terms of efficiency, the results highlight that the [OMMIM][SCN] system is more energy efficient when IL inlet temperature increases. However, its efficiency declines at higher absorption pressure, whereas the energy efficiency of the [BMMIM][TF2N] system remains constant. As for the exergy efficiency,

the [OMMIM][SCN] system shows higher exergy efficiency than [BMMIM][TF2N] throughout the studied temperature and pressure ranges. However, a decline in exergy efficiency is observed beyond the peak point temperature range of 50-60°C. This indicates that [OMMIM][SCN] exhibits better performance than established IL [BMMIM][TF2N], confirming its potential as a promising alternative for large-scale pre-combustion CO_2 capture process for blue H_2 production. However, while computational toxicity predictions using ADMETlab 2.0 provide valuable insights, experimental validation of [OMMIM][SCN] is crucial to evaluate its practical feasibility in industrial applications. In addition to toxicity assessment, further evaluation encompassing scalability and cost should be addressed to determine its large-scale implementation. Also, additional study is needed to optimize the [OMMIM][SCN] system to reduce irreversibility in process equipment and increase energy efficiency.

ACKNOWLEDGEMENTS

The authors acknowledge the paper was made possible by grant QUHI-CENG-22-23-465 from Qatar University. The statements made herein are solely the responsibility of the author[s].

REFERENCES

1. P. R. Yaashikaa, P. Senthil Kumar, S. J. Varjani, and A. Saravanan, "A review on photochemical, biochemical and electrochemical transformation of CO2 into value-added products," *J. CO2 Util.*, vol. 33, no. May, pp. 131–147, 2019, doi: 10.1016/j.jcou.2019.05.017.
2. F. Birol, "The Future of Hydrogen – Analysis - IEA," *Technology report*, 2019. https://www.iea.org/reports/the-future-of-hydrogen (accessed Mar. 13, 2021).
3. C. E. Regulator, "Market Snapshot: How hydrogen has the potential to reduce the CO2 emissions of natural gas," *Canada Energy Regulator*, 2020. https://www.cer-rec.gc.ca/en/data-analysis/energy-markets/market-snapshots/2020/market-snapshot-hydrogen-potential.html (accessed Nov. 19, 2022).
4. M. Aghaie, N. Rezaei, and S. Zendehboudi, "A systematic review on CO 2 capture with ionic liquids : Current status and future prospects," vol. 96, no. December 2017, pp. 502–525, 2018, doi: 10.1016/j.rser.2018.07.004.
5. S. Mohammed, F. Eljack, M. K. Kazi, and M. Atilhan, "Development of a deep learning-based group contribution framework for targeted design of ionic liquids," *Comput. Chem. Eng.*, vol. 186, no. January, p. 108715, 2024, doi: 10.1016/j.compchemeng.2024.108715.
6. S. Mohammed, F. Eljack, S. Al-Sobhi, and M. K. Kazi, "Simulation and 3E assessment of pre-combustion CO2 capture process using novel Ionic liquids for blue H2 production," *Comput. Aided Chem. Eng.*, vol. 53, pp. 517–522, Jan. 2024, doi: 10.1016/B978-0-443-28824-1.50087-9.
7. G. Xiong *et al.*, "ADMETlab 2.0: An integrated online platform for accurate and comprehensive predictions of ADMET properties," *Nucleic Acids Res.*, vol. 49, no. W1, pp. W5–W14, 2021, doi: 10.1093/nar/gkab255.
8. DOE/NETL, "IEAGHG Techno - Economic Evaluation of SMR Based Standalone (Merchant) Hydrogen Plant with CCS, 2017," 2022. [Online]. Available: https://eur-lex.europa.eu/legal-content/EN/TXT/?uri=CELEX:52020DC0301%0Ahttp://www.irena.org/publications%0Ahttp://ieaghg.org/exco_docs/2017-02.pdf.
9. D. Hospital-Benito, I. Díaz, and J. Palomar, "Technical performance and environmental assessment of an ionic liquid-based CCS process for hydrogen production," *Sustain. Prod. Consum.*, vol. 38, no. May, pp. 283–294, 2023, doi: 10.1016/j.spc.2023.04.017.
10. H. Alyasi, A. AlNouss, Y. Bicer, and G. Mckay, "A biomass-based integrated energy system for urea and power production: Thermodynamic analysis," *Int. J. Hydrogen Energy*, vol. 91, no. October, pp. 1365–1375, 2024, doi: 10.1016/j.ijhydene.2024.10.113.